Physical, Mechanical, and Antibacterial Properties of Chitosan/PEO Blend Films

Svetlana Zivanovic,*,† Jiajie Li,† P. Michael Davidson,† and Kevin Kit‡

Food Biopolymers Research Group, Department of Food Science and Technology, University of Tennessee, 2509 River Drive, Knoxville, Tennessee 37996, and Department of Material Science and Engineering, University of Tennessee, Knoxville, Tennessee 37996

Received December 1, 2006; Revised Manuscript Received February 13, 2007

Films formed by blending of two polymers usually have modified physical and mechanical properties compared to films made of the individual components. Our preliminary studies indicated that incorporation of chitosan in polyethylene oxide (PEO) films may provide additional functionality to the PEO films and may decrease their tendency to spherulitic crystallization. The objective of this study was to determine the correlation between chitosan/PEO weight ratio and the physical, mechanical, and antibacterial properties of corresponding films. Films with chitosan/PEO weight ratios from 100/0 to 50/50 in 10% increments were characterized by measuring thickness, puncture strength (PS), tensile strength (TS), elongation at break (%*E*), water vapor permeability (WVP), and water solubility (WS). Additionally, the films were examined by polarized microscopy, wide-angle X-ray diffraction (WAXD), and Fourier transform infrared (FTIR) spectroscopy, and their antibacterial properties were tested against *Escherichia coli*. The chitosan fraction contributes to antimicrobial effect of the films, decreases tendency to spherulitic crystallization of PEO, and enhances puncture and tensile strength of the films, while addition of the PEO results in thinner films with lower water vapor permeability. Films with 90/10 blend ratio of chitosan/PEO showed the most satisfactory PS, TS, %*E*, and antibacterial properties of all tested ratios.

1. Introduction

There has been a growing interest over the past few years in the development of biopolymers partly because of their renewable, sustainable, and biodegradable properties. As one of the candidates for such biopolymers, chitosan has attracted much attention mainly because of its antimicrobial and metal-binding properties. Chitosan is a cationic biopolymer obtained by a full or partial N-deacetylation of chitin, which is known to be the second most abundant biopolymer in nature and is the major component of the exoskeleton of crustaceans.[1] Chitosan may be regarded as a binary heteropolysaccharide containing $\beta(1-4)$ linked 2-acetamido-2-deoxy-β-D-glucopyranose and 2-amino-2-deoxy-β-d-glucopyranose residues.[2] Chitosan has been evaluated for various uses in the food, medical, pharmaceutical, agricultural, and chemical industries because of its nontoxic, biocompatible, mucoadhesive, and biodegradable properties.[2−4] Dissolved chitosan has antimicrobial and metal-binding properties and has been used as an antimicrobial additive to bind metals from food-processing wastewaters.[5−7] In addition, because of its free amino groups, chitosan can be dissolved in acidic aqueous solutions and form gels, films, sutures, beads, and fibers.[2]

Polyethylene oxide (PEO) is a synthetic uncharged polymer with a molecular formula $(-CH_2CH_2O-)_n$. It is low-toxic, semicrystalline, bioadhesive, and mucoadhesive because of its water solubility, hydrophilicity, high viscosity, ability to form hydrogen bonds, and biocompatibility with other bioactive substance. PEO has been widely used in a variety of dosage forms in the pharmaceutical industry such as for the production of hot-melt extruded capsules. However, since PEO is a flexible-chain polymer, pure PEO films have relatively poor mechanical and physical characteristics and high water solubility which limit their application. A convenient and effective method to improve PEO film properties is blending PEO with other polymers. The films formed by blending two or more polymers usually result in modified physical and mechanical properties compared to films made of the individual components. It has been reported that starch−chitosan blend films exhibited a higher flexibility and improved the percentage elongation than films produced from single polymers.[8] The blend of chitosan and quaternized poly(4-vinyl-*N*-butyl)pyridine showed stronger tensile strength and breaking elongation than films of pure chitosan.[9]

Chitosan/PEO blend films may provide additional functionality compared to the pure polymer films. Chitosan may improve mechanical properties and decreased water solubility of the PEO films, while PEO may contribute to the formation of colorless films that are more flexible. Our preliminary data showed that films with chitosan content of more than 50% decreased the PEO tendency to spherulitic crystallization. Therefore, the objective of this research was to evaluate the physical, mechanical, and antibacterial properties of films composed of blends of low molecular weight chitosan and high molecular weight PEO.

2. Materials and Methods

Materials. Chitosan of low molecular weight (~150 kDa) with a degree of deacetylation above 85% and PEO of high molecular weight (~900 kDa) were purchased from Aldrich Chemical Co. (Milwaukee, WI).

Film Preparation. Mixtures of chitosan and PEO with different weight ratios (100/0, 90/10, 80/20, 70/30, 60/40, 50/50) were dissolved in 1% w/w acetic acid and were stirred overnight at room temperature.

* To whom correspondence should be addressed. Tel.: 865-974-0844; fax: 865-974-7332; e-mail: lanaz@utk.edu.

† Department of Food Science and Technology.

‡ Department of Material Science and Engineering.

10.1021/bm061140p CCC: $37.00
Published on Web 03/28/2007

The film-forming solutions, regardless on the chitosan/PEO ratio, contained 1% w/w polymer solids in 1% w/w acetic acid. After filtration through miracloth (Calbiochem-Novabiochem Corp., San Diego, CA), 10 g of film-forming solutions was poured into 50-mm-diameter polystyrene petri dishes, and the solvent was evaporated in a vacuum oven at 38 °C under 17 kPa pressure for 24 h. The dried films were peeled from the Petri dishes and were kept in desiccators at 20% relative humidity at room temperature.

Thickness. Film thickness (μm) was determined on six films per ratio treatment averaging measurements at five points for each film using a hand-held microcaliper (Mitutoyo Corp, Kawasaki, Kanagawa, Japan). Similarly, thickness measurements were taken for films used for determination of water vapor permeability, puncture strength, and tensile strength, and the values were accordingly calculated.

Film Crystallization. Crystallization of polymers in the films was monitored by a polarized microscope (Olympus-BX51, Melville, NY). Films were observed under polarized microscope with 100× magnification within 24 h after casting. X-ray diffractometer was used to inspect the diffractograms of the films at ambient temperature. It was conducted using a Molecular Metrology small-angle X-ray scattering (SAXS)/wide-angle X-ray diffraction (WAXD) system equipped with a monochromic CuKα (1.5418 Å) X-ray source, a three-pinhole alignment, and two-dimensional detector operating at 45 kV and 0.66 mA with the beam size of 30 μm. The WAXD patterns were recorded on reusable Fuji image plates with the sample-to-film distance of 36.52 mm. The image plate was scanned in a Fuji X BAS-1800II image analyzer and the resultant image was converted to intensity versus 2θ or q plot using Polar X-ray analysis software. The data were collected over an angular range from 5° to 40° 2θ in a continuous mode. Relative crystallinity percentage (X_c) of the films were calculated by the following equation:[10]

$$X_c = [A_c/(A_c + A_a)] \times 100\%$$

where A_c and A_a are the areas of the crystalline and amorphous regions, respectively.

Film Mechanical Properties. The mechanical properties were determined using a TA.XT*plus* Texture Analyzer (Texture Technologies Corp., Scarsdale, NY/Stable Micro Systems, Godalming, Surrey, U.K.). Puncture strength (PS) was measured on three films per ratio treatment using the TA-108S fixture and 2-mm-diameter needle probe (TA-52) moving with a test speed of 1 mm/s. The PS was calculated by dividing the maximum force at break (N) by the thickness (mm) at the broken areas. Tensile strength (TS) and percent elongation at break (%E) were based on the ASTM D882 method.[11] Film specimens per ratio treatment were cut by Specimen cutting die (Qualitest USA LC, Plantation, FL) to the strips with uniform width of 6 mm and were tested by using a double clamp (TA-96) at a test speed of 1 mm/s. Initial grip separation was set as 20 mm. The TS was expressed in MPa and was calculated by dividing the maximum load (N) by the cross-sectional area (m^2). Percent elongation at break was determined by dividing the extension at the moment of rupture by the initial gauge length of the samples and multiplying by 100. PS, TS, and %E measurements were replicated three times for each type of film.

Water Solubility. The dried films were immersed in 40 mL methanol for 24 h to remove acetic acid existing in the films and then were taken out and dried in the vacuum oven for 24 h at room temperature. The dried films were weighed (W_1), were immersed in distilled water for 24 h, were dried in a vacuum oven for 24 h at room temperature, and then were stored in a desiccator for 5 h for weight balance. The equilibrium weights of the films were weighed (W_2). Water solubility was calculated as the following equation:

$$W_s = (W_1 - W_2)/W_1 \times 100\%$$

Water Vapor Permeability. Water vapor permeability (WVP) was measured gravimetrically using ASTM E-96 method and was calculated using the WVP correction method described by Gennadios et al.[12,13] Fisher permeability cups (Fisher Scientific, Pittsburgh, PA) filled with 5 mL distilled water were sealed by the tested films. Silicon sealant (High Vacuum Grease, Dow Corning, Midland, MI) and the ring covers with three screws around the cup circumference were used for attaching the films to the cups tightly. After measuring the initial weight, the cups were placed in an environment chamber (Yamato Scientific America, INC., Orangeburg, NY) equipped with a fan for air circulation and set at 25 °C and 50% R.H. Steady state was obtained after 2 h and cups were weighed five times at 1-h intervals. Linear regression analysis of the weight loss versus time curves was performed to obtain the accurate steady-state slopes from which the actual film WVP values were calculated.

Table 1. Thickness of Chitosan/PEO Blend Films with Weight Ratio from 100/0 to 50/50[a]

film (w/w chitosan/PEO)	thickness (μm)
100/0	38.1 ± 4.1^b
90/10	44.6 ± 1.7^a
80/20	34.5 ± 0.6^c
70/30	30.2 ± 0.6^d
60/40	29.4 ± 1.2^d
50/50	25.4 ± 1.2^e

[a] Values reported are means and standard deviation. Superscript letters indicate significant difference at $p < 0.05$ by LSD test (SAS, 2000).

FTIR Analysis. Fourier transform infrared (FTIR) measurements were performed to evaluate the uniformity of the film surfaces. This spectrum of the films was recorded using FTIR-ATR (Nexus 680, Thermo Nicolet Corp, Madison, WI) with the wavenumber range 500−4000 cm^{-1}. Film uniformity was assessed by observing both top and bottom sides of the same films.

Antibacterial Property in the Liquid System. *Escherichia coli* K-12, the test microorganism, was grown in brain heart infusion (BHI; Difco) broth for 48 h at 35 °C. Test films of 50-mm diameter were submerged into culture tubes containing 9 mL sterile phosphate buffer (0.05 M, pH = 7.08) inoculated with ca. 10^6 colony-forming unit (CFU)/mL bacteria, were mixed by vortexing, and were incubated for 6 h at 25 °C. Phosphate buffer with the same *E. coli* K-12 inoculum but with no film was used as positive control and phosphate buffer with film but no inoculum was the negative control. The survival of *E. coli* K-12 was determined using the pour-plate method on trypticase soy agar (TSA) medium.[14] All measurements were performed with three replications.

Statistical Analysis. All measurements were done in triplicate with individually prepared films as the replicated experimental units. Significant differences between two groups were determined using least significant difference (LSD) test in the SAS program (SAS, 2000).

3. Results and Discussion

3.1. Appearance and Thickness. All tested films were transparent. The films with chitosan/PEO ratios of 100/0 and 90/10 had slightly yellowish color, but as the fraction of PEO increased, the 80/20 to 50/50 films became colorless. Our previous research indicated that more than 50% PEO resulted in opacity of the films because of the spherulitic crystallization characteristics of PEO.

Thickness of the films is shown in Table 1. Thickness ranged from 25.4 ± 1.2 μm for 50/50 blend ratio to 44.6 ± 1.7 μm for 90/10 blend ratio, indicating that thickness of the films significantly increased ($p < 0.05$) with increase of chitosan content in the blend.

3.2. Film Crystallization. Since PEO is a semicrystalline polymer, it is necessary to study its crystallization within the films as it may affect structure and physical properties of the

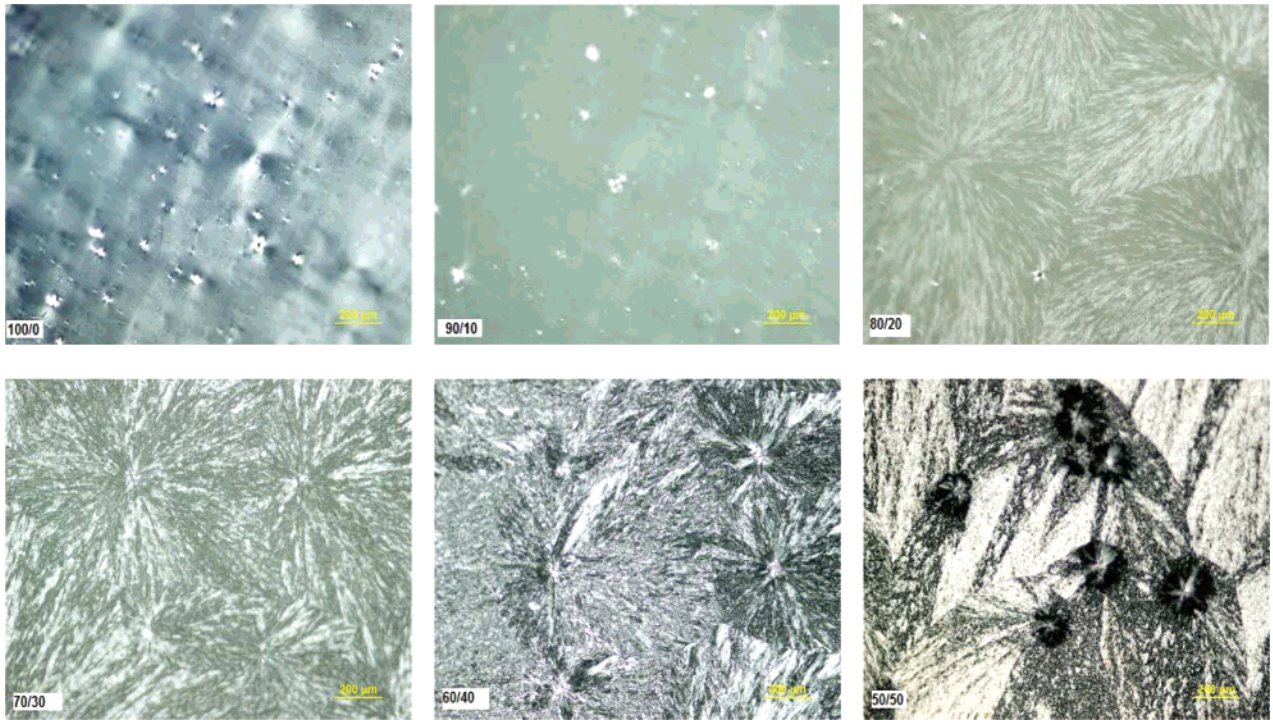

Figure 1. Polarized micrographs of films with chitosan/PEO blend ratios of 100/0, 90/10, 80/20, 70/30, 60/40, and 50/50 with 100× magnification within 24 h after casting. Scale bar: 200 μm.

films. Figure 1 illustrates the shape and distribution of the crystals within the films as observed under polarized microscope with 100× magnification. The PEO crystals are easily recognized because of monoclinic unit cells of crystals with four radially oriented PEO chains. As shown in Figure 1, the increase of chitosan fraction in the films reduced spherulitic crystallization of PEO and no crystallization was observed in the films with 90/10 blend ratio.

Wide-angle X-ray diffraction (WAXD) patterns of 100/0 to 50/50 chitosan/PEO blend films are presented in Figure 2. The corresponding diffraction angle (2θ) and relative crystallinity percentage (X_c) are listed in Table 2. The diffractogram of both 100/0 and 90/10 films did not show characteristic peaks but a broad hump in the range of 10−40° 2θ, which indicated a predominantly amorphous form of the chitosan in the films (Figure 2A, 2B). In contrast, all of the diffraction patterns of 80/20 to 50/50 chitosan/PEO blend films showed two sharp peaks with the highest intensity at 19.0° and 23.3° 2θ, resulting from PEO crystals (Figure 2C−F). As expected, the crystallinity of the films from 80/20 to 50/50 blend ratio increased significantly having the value of X_c increasing from 14.9% to 83.9%, respectively. The reduction in PEO crystallization by chitosan is probably a result of interruption of PEO−PEO interactions because of formation of hydrogen bonds between ether and amino groups from PEO and chitosan, respectively. Our results of X-ray diffraction analysis confirmed that 90% or more chitosan inhibits the crystallization of PEO in the cast films while the clear phase separation happens when chitosan content is 80% or less.

3.3. Film Mechanical Properties. The results for puncture strength (PS), tensile strength (TS), and elongation at break (%E) for films with different chitosan/PEO blend ratios are shown in Table 3. The PS of the film increased from 158.9 ± 17.0 N/mm for 50/50 blend ratio to 416.0 ± 24.7 N/mm for 100/0 blend ratio. Interestingly, the PS increased significantly as the chitosan fraction increased from 50 to 80%, but there was no significant difference in the puncture strength among the films with 80% and more chitosan. Therefore, it appears that the addition of minimum 80% chitosan would be needed to increase the puncture strength of the blend films.

Similarly to PS, TS values increased from 47.0 ± 8.8 MPa for 50/50 films to 73.5 ± 7.1 MPa for 100/0 films. The TS of 90/10 chitosan/PEO films was similar to TS of pure chitosan films, but with 20% or more PEO in the blend, the tensile strength of the films decreased relatively to the PEO fraction. Compared to the TS values of the widely used plastic films, such as LDPE and HDPE with values of 23.6 and 47.4 MPa, respectively,[11] the chitosan/PEO films retained good tensile strength.

Mean values for the elongation at break (%E) are also presented in Table 3. The results indicated that addition of PEO to the blend reduced extensibility of the films, creating more brittle products. Compared to the elongation values of LDPE and HDPE of 205% and 570%, respectively,[11] all the chitosan/PEO films exhibited poor elongation of 4.2 ± 1.4% for 50/50 films to 17.7 ± 13.3% for 100/0 films. Since crystallinity development of PEO in the films may be the main reason for impaired elongation, further studies will examine effects of molecular weight of PEO and chitosan as well as film-forming conditions on extensibility of the blend films.

3.4. Water Solubility. The results for water solubility of chitosan/PEO blend films are shown in Figure 3. Chitosan is soluble in dilute aqueous acidic solution (pH < 6.5) but is insoluble in pure water, while PEO is water-soluble polymer. Although all the films maintained the original shape after being immersed in water for 24 h at room temperature, the 50/50 films dissolved the most, 46.6 ± 0.5%. However, with the increase of chitosan content, the water solubility significantly decreased, with only a 0.9 ± 1.0% loss for 100/0 films ($p < 0.05$). Although high water resistance of plastic films may be desired for many industrial applications, controlled solubility of biodegradable films offers advantages for use in the food, pharmaceutical, and agricultural industries. For example, it has been reported that microporous chitosan/PEO membranes can

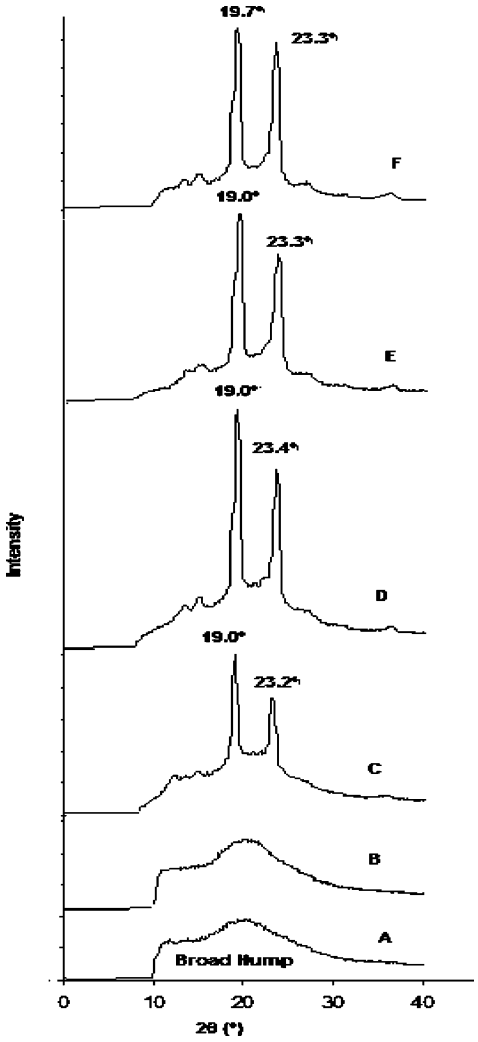

Figure 2. 2θ-scan wide-angle X-ray diffraction (WAXD) patterns of films with chitosan/PEO blend ratio of (A) 100/0, (B) 90/10, (C) 80/20, (D) 70/30, (E) 60/40, and (F) 50/50.

Table 2. Diffraction Angle (2θ) of Sharp Peaks and Relative Crystallinity Percentage (X_c) of the Chitosan/PEO Blend Films with Weight Ratio from 100/0 to 50/50

film (w/w chitosan/PEO)	peak I (°)	peak II (°)	X_c(%)
100/0	a	a	a
90/10	a	a	a
80/20	19.0	23.2	14.9
70/30	19.0	23.4	28.7
60/40	19.0	23.3	36.7
50/50	19.7	23.3	83.7

[a] Indicates there is no readable crystalline peak.

control rate of drug release by stepwise solubilization of PEO in water and by altering the mesh size of the membranes.[15]

3.5. Water Vapor Permeability. As shown in Figure 4, WVP was significantly affected by the ratio of the polymers from 23.49 ± 6.39 g mm/kPa h m^2 for 90/10 chitosan/PEO films to 6.20 ± 0.72 g mm/kPa h m^2 for 50/50 films. Interestingly, films with 30% or more PEO had similar and unexpectedly low WVP values compared to films with high chitosan content.

As suggested by Gontard and Guilbert, water vapor transmission through a hydrophilic film depends on solubility and diffusivity of water molecules in the film matrix.[16] However, although the increase of the PEO fraction enhanced the solubility of the films, it did not cause higher permeability, which indicates

Table 3. Puncture Strength (PS), Tensile Strength (TS), and Elongation at Break (%E) of the Chitosan/PEO Blend Films with Weight Ratio from 100/0 to 50/50[a]

film (w/w chitosan/PEO)	PS (N/mm)	TS (MPa)	elongation (%)
100/0	416.0 ± 24.7^a	73.5 ± 7.1^a	17.7 ± 13.3^a
90/10	416.2 ± 54.9^a	67.0 ± 2.3^{ab}	11.1 ± 4.2^{ab}
80/20	441.0 ± 21.6^a	55.4 ± 14.6^{bc}	10.8 ± 5.0^{ab}
70/30	324.7 ± 31.8^b	52.7 ± 9.8^{bc}	8.0 ± 4.5^{ab}
60/40	269.8 ± 6.3^c	54.3 ± 3.8^{bc}	8.1 ± 2.6^{ab}
50/50	158.9 ± 17.0^d	47.0 ± 8.8^c	4.2 ± 1.4^b

[a] Means of three replicates ± standard deviation. The means in the same column followed by the same letter are not significantly different ($p > 0.05$) by LSD test.

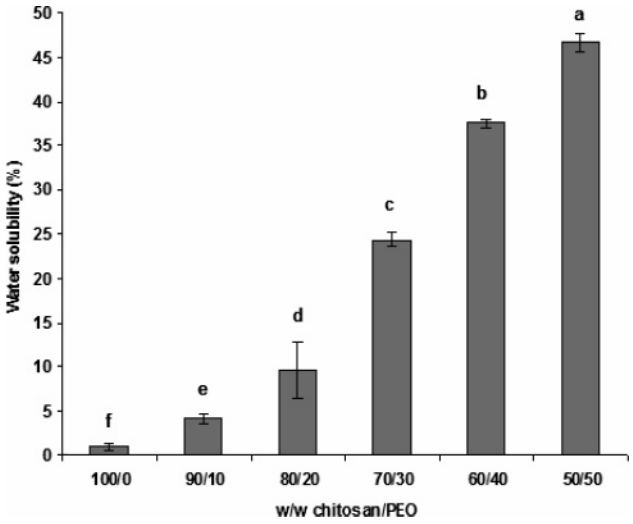

Figure 3. Effect of chitosan/PEO blend ratio from 100/0 to 50/50 on water solubility of the corresponding films. Error bars represent standard deviation ($n = 3$). Letters indicate significant difference at $p < 0.05$.

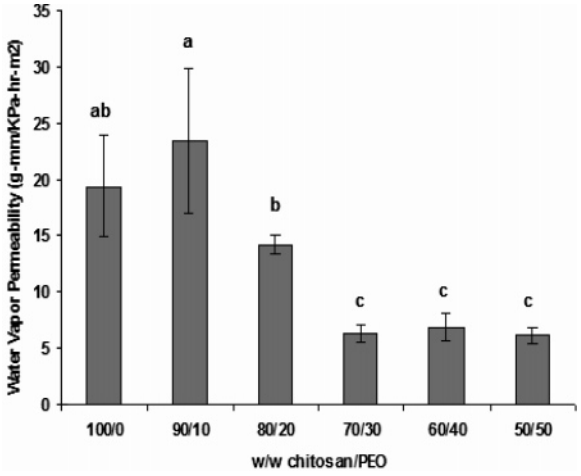

Figure 4. Effect of chitosan/PEO blend ratio from 100/0 to 50/50 on water vapor permeability of the corresponding films in the environmental chamber at 25 °C and 50% R.H. Error bars represent standard deviation ($n = 3$). Letters indicate significant difference at $p < 0.05$.

that the main factor in water vapor permeability is diffusivity of water molecules through the film matrix. The impeded diffusivity could be due to promotion of strong intermolecular interactions between chitosan and PEO molecules which decreased intermolecular distance resulting in more compact films or crystallinity of PEO that caused the percolation of water molecules around the insoluble crystals resulting in longer

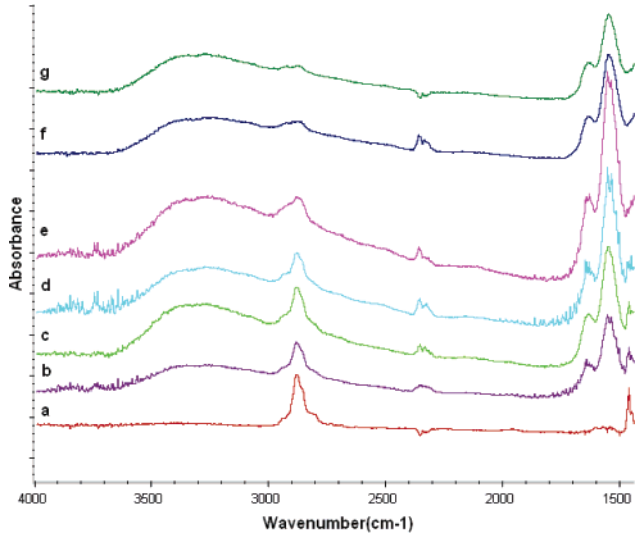

Figure 5. A portion (4000−1500 cm^{-1}) of FTIR spectra of chitosan/PEO blend films with ratio (a) 0/100, (b) 50/50, (c) 60/40, (d) 70/30, (e) 80/20, (f) 90/10, and (g) 100/0. All spectra are plotted in absorbance mode.

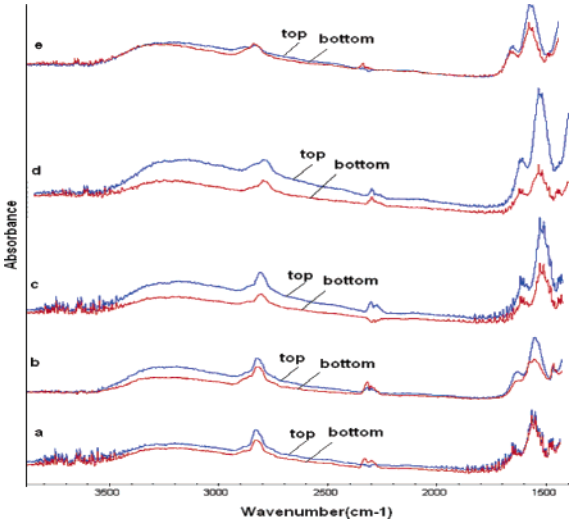

Figure 6. A portion (4000−1500 cm^{-1}) of FTIR spectra of chitosan/PEO blend films with ratio (a) 50/50, (b) 60/40, (c) 70/30, (d) 80/20, and (e) 90/10, observed on both top and bottom sides on an identical point.

diffusion paths. On the other hand, the water vapor permeability changed with film thickness. The films with 90/10 chitosan/PEO ratio had the highest WVP value partly because these were the thickest films. McHugh et al. have reported that positive relationships exist between thickness and WVP since the increased film thickness could increase the relative humidity in vicinity of the films and alter the water sorption kinetics.[17] These results indicate that the diffusion of our polymer-blended films shows non-Fickian behavior.[18]

3.6. FTIR Analysis. FTIR spectra of chitosan/PEO films are shown in Figure 5. Pure PEO (0/100) films were used for comparison. Four characteristic absorption bands of pure chitosan films are as follows (Figure 5g): (1) a broad band at around 3500−3100 cm^{-1} attributed to N−H and OH···O stretching vibration, as well as intermolecular hydrogen bonding of chitosan molecules,[19,20] (2) a very weak band at 2884 cm^{-1} from CH stretch, (3) the one at 1655 cm^{-1} was due to the amide I,[21] and (4) the amine−NH_2 absorption band (amide II) at around 1550 cm^{-1}.[22] As to the pure PEO film (Figure 5a), the typical absorption band is at 2885 cm^{-1} attributed to the CH_2 stretching vibration,[22] which can overlap with that of chitosan. Since a high molecular weight (900 kDa) PEO was used, absorption bands of hydroxyl groups from PEO could be considered negligible in the spectra.[23] With the increase of PEO content, the absorbance intensity of CH_2 stretching vibration at 2885 cm^{-1} increased and absorbance intensity of $-NH_2$ stretching at around 1558 cm^{-1} decreased. However, there is no strong evidence, such as the shift of the absorption bands, to establish a clear hypothesis for the intermolecular interaction between chitosan and PEO with the weight ratio change.

To detect the surface composition and to evaluate stability of the cast films, the films were observed from top and bottom side by FTIR spectroscopy (Figure 6). In films with less than 50% PEO, chitosan was apparently oriented toward the top side of the films and PEO toward the bottom side, while in 50/50 films the FTIR scans were almost the same.

3.7. Antibacterial Property in the Liquid System. As shown in Table 4, all mixtures of chitosan/PEO films reduced the number of *E. coli* K-12 by approximately 3 log CFU/mL from the positive control of 9.63 log CFU/mL in 6 h. This indicated that the chitosan/PEO films had satisfactory antibacterial properties. As expected, the antibacterial activity of the films was approximately proportional to chitosan fraction. Thus, a 3.10 log CFU/mL reduction was observed for 90/10 and 2.54 log CFU/mL for 60/40 chitosan/PEO blend ratio. However, 50/50 chitosan/PEO films showed a strong antibacterial activity with reduction in viable cells of 3.27 log CFU/mL which was similar to that of 100/0 chitosan/PEO films ($p < 0.05$). This may be explained by the compatibility of chitosan/PEO blends. As we discussed earlier, the phase separation may start when concentration of PEO is 20% or more. With the increased content of PEO (80/20 to 60/40 films), the distribution of PEO crystals on the surface of the films may decrease the possibility of interaction of chitosan with *E. coli* K-12 and reduce lethality of the films. However, as suggested by Zhao et al., the compatibility of chitosan/PEO blends is closely related to the composition and chitosan and PEO may become miscible again at 50% or less chitosan.[24] As for the 50/50 blend ratio, chitosan and PEO are miscible and chitosan molecule chains would have more chance to combine with and kill the bacteria than from immiscible films. Further investigations on structure are in progress.

Table 4. Inhibitory Effects of Chitosan/PEO Blend Films toward *Escherichia coli* K-12 Inoculated in Sterile Phosphate Buffer (0.05 M, pH = 7.08) and Stored for 6 h at 25 °C[b]

film (w/w chitosan/PEO)	*surviving E. coli* K12 (Log_{10} CFU[a]/mL)	*E. coli* K12 reduction (Log_{10} CFU/mL)	pH in negative control tubes after 6 h
positive control (no film)	9.63 ± 0.09	0	7.08
100/0	6.20 ± 0.07[e]	3.43	6.57
90/10	6.53 ± 0.26[cd]	3.10	6.84
80/20	6.77 ± 0.15[bc]	2.86	6.85
70/30	6.86 ± 0.27[ab]	2.77	6.87
60/40	7.09 ± 0.04[a]	2.54	7.00
50/50	6.36 ± 0.10[de]	3.27	7.01

[a] CFU = colony-forming unit. [b] Means of three replicates ± standard deviation. The means in the same column followed by the same letter are not significantly different ($p > 0.05$) by LSD test.

4. Conclusions

Films formed by blending of chitosan and PEO have altered properties than films produced from either polymer alone. The chitosan fraction contributes to antimicrobial effect of the films, decreases tendency to spherulitic crystallization of PEO, and enhances puncture and tensile strength of the films, while addition of the PEO results in thinner films with lower water vapor permeability.

Films with 90/10 blend ratio of chitosan/PEO exhibited the best mechanical properties (puncture and tensile strength), no crystallization, high water vapor permeability, and significant antibacterial effect. On the basis of our results, chitosan/PEO blend films have the potential to be used in the food industry as active packaging materials to inhibit food-borne pathogens and in the pharmaceutical industry for controlled release of active components. The future study will be focused on evaluation of film-forming techniques on mechanical, physical, and antimicrobial properties of spin-coated chitosan/PEO films.

Acknowledgment. This research was funded by U.S. EPA Science To Achieve Results (STAR) program grant #GR832372 and Hatch fund from the Tennessee Experiment Station TEN264.

References and Notes

(1) Roberts, G. A. F. *Chitin Chemistry*; The MacMillan Press Ltd.: London, 1992.
(2) Angelova, N.; Manolova, N.; Rashkov, I. *J. Bioact. Compat. Polym.* **1995**, *10*, 285−298.
(3) Zivanovic, S.; Chi, S.; Draughon, A. E. *J. Food Sci.* **2005**, *70*, 45−51.
(4) Agnihotri, S. A.; Mallikarjuna, N. N.; Aminabhavi, T. M. *J. Controlled Release* **2004**, *100*, 5−28.
(5) Selmer-Olsen, E.; Ratnaweera, H. C.; Pehrson, R. R. *Waste Water Technol.* **1996**, *34*, 33−40.
(6) Sudarshan, N. R.; Hoover, D. G.; Knorr, D. *Food Biotechnol.* **1992**, *6*, 257−272.
(7) Zivanovic, S.; Basurto, C. C.; Chi, S.; Davidson, P. M.; Weiss, J. *J. Food Prot.* **2004**, *67*, 952−959.
(8) Mathew, S.; Brahmakumar, M.; Abraham, T. E. *Biopolymers* **2006**, *82*, 176−187.
(9) Liu, C. H.; Xiao, C. B. *J. Appl. Polym. Sci.* **2004**, *92*, 559−566.
(10) Helander, I. M.; Nurmiaho-Lassila, E. L.; Ahvenainen, R.; Rhoades, J.; Roller, S. *Int. J. Food Microbiol.* **2001**, *71*, 235−244.
(11) *Standard test method for tensile properties of thin plastic sheeting*; Philadelphia, PA, 2002.
(12) *Standard test method for water vapor transmission of materials*; Philadelphia, PA, 2002.
(13) Gennadios, A.; Weller, C. L.; Gooding, C. H. *J. Food Eng.* **1994**, *21*, 395.
(14) Swanson, K. M. J.; Petran, R. L.; Hanlin, J. H. *Culture Methods for Enumeration of Microorganisms*; American Public Health Association: Washington, DC, 2001.
(15) Jin, J.; Song, M. *J. Appl. Polym. Sci.* **2006**, *102*, 436−444.
(16) Gontard, N.; Guilbert, S. *Food Packaging and Preservation*; Blackie Academic & Professional: London, 1994.
(17) McHugh, T. H.; Avena-Bustillos, R.; Krochta, J. M. *J. Food Sci.* **1993**, *58*, 899−903.
(18) Crank, J. *The Mathematics of Diffusion*; Oxford University Press: 1975.
(19) de Vasconcelos, C. L.; Bezerril, P. M.; dos Santos, D. E. S.; Dantas, T. N. C.; Pereira, M. R.; Fonseca, J. L. C. *Biomacromolecules* **2006**, *7*, 1245−1252.
(20) Jiang, H.; Liang, J.; Grang, J. T.; Su, W.; Bunning, T. J.; Cooper, T. M.; Adams, W. W. *Macromol. Chem. Phys.* **1997**, *198*, 1561−1578.
(21) Wan, Y.; Wu, H.; Yu, A. X.; Wen, D. J. *Biomacromolecules* **2006**, *7*, 1362−1372.
(22) Duan, B.; Dong, C.; Yuan, X.; Yao, K. *J. Biomater. Sci., Polym. E* **2004**, *15*, 797−811.
(23) Sawatari, C.; Kondo, T. *Macromolecules* **1999**, *32*, 1949−1955.
(24) Zhao, W.; Yu, L.; Zhong, X.; Zhang, Y.; Sun, J. *J. Macromol. Sci. Phys.* **1995**, *34*, 231−237.

BM061140P